The Structure of the Nucleons

G. G. Simon, F. Borkowski, Ch. Schmitt, and V. H. Walther
Institut für Kernphysik, Universität Mainz

Z. Naturforsch. **35a**, 1–8 (1980); received October 2, 1979

Dedicated to Professor H. Hintenberger on the occasion of his 70th birthday

Electron-proton and electron-deuteron scattering experiments in a wide four momentum range provide information about the structure of the proton and the neutron. The structure is a direct consequence of the hadronic interaction of the nucleon and reveals properties of the strong interaction. Absolute differential cross sections can be expressed in terms of electromagnetic form factors which lead to an understanding of the coupling mechanism between the electromagnetic field and the strongly interacting hadron. The structure can also be discussed in terms of charge densities, but this analysis is strongly restricted by recoil effects. The charge rms radius extracted from recent measurements is higher in the case of the proton than that derived from former fits. The higher value of the charge rms radius of the proton is in excellent agreement with the latest Lamb shift measurements.

I. Introduction

During the past 25 years many different experiments have provided convincing evidence that nucleons have a structure. This structure is a direct consequence of the hadronic interaction and reveals highly valuable information about the dynamics of the strong interaction. The interpretation of the extended nucleon in terms of the spatial charge distribution has only a pictorial usefulness, however, it is useful for some calculations in nuclear physics. Today there is theoretical consensus that the nucleon is a composed object. A very successful method to describe the structure is to imagine the nucleon as being composed of a certain number of mesons and heavier hadrons. Moreover, on the other hand experiments in high energy physics provide the description of the electromagnetic structure of the nucleon by a superposition of the wave functions of three quarks. There does not exist a generally valid model for an interpretation of the experimental observations; thus there exist different methods to analyse the experimental data (Ref. [1, 2, 3, 4]).

A very successful tool to study the structure of the nucleons is the elastic scattering of relativistic electrons. Such experiments have been performed for a long time. The better accuracy of the experimental methods of today as well as the extension to higher momentum transfers has yielded new information. Absolute cross sections at low momentum transfer have been determined with a small normalization error of 0.5% (Ref. [5, 6]). These data are very crucial for the determination of the root mean squared charge radius $\langle r^2\rangle^{1/2}$ of the nucleon. On the other hand, experiments at very high momentum transfer up to $q^2 = 600\ \mathrm{fm}^{-2}$ are useful for a good spatial resolution of the charge distribution (0.05 fm). Furthermore, the recent experiments in the whole q region revealed the hadronic structure and led to an understanding of the coupling mechanism between the electromagnetically interacting virtual photon and the strongly interacting hadron. The data for large q values support the quark model, which favors a q^{-4} dependence of the nucleon form factors.

Reprint requests to Prof. V. H. Walther, Institut für Kernphysik, Universität Mainz, D-6500 Mainz.

II. Electron-Nucleon Scattering: General Considerations

1. Electron-Proton Scattering

The ratio of the measured cross section to the cross section for the scattering of a Dirac electron on a spinless pointlike charge contains all the information about the nucleon structure. For electron nucleon scattering we have no pure Coulomb interaction. The cross section for the elastic scattering on the proton for a single photon exchange including all interaction effects is given by the Rosenbluth formula

$$\frac{\mathrm{d}\sigma/\mathrm{d}\Omega_{\mathrm{exp}}}{\mathrm{d}\sigma/\mathrm{d}\Omega_{\mathrm{NS}}} = A(q^2) + B(q^2)\cdot\tan^2\frac{\Theta}{2} \qquad (1)$$

0340-4811 / 80 / 0100-0001 $ 01.00/0. — Please order a reprint rather than making your own copy.

where Θ is the scattering angle in the laboratory system. The structure functions $A(q^2)$ and $B(q^2)$ contain two form factors which are functions only of q^2, the squared four momentum transfer carried by the exchanged photon, if all particles are on the mass shell. We want to emphasize, that all the information about the structure of the nucleons is contained completely in the q^2 dependence of these form factors. The evaluation of the form factors from the cross sections occurs via Rosenbluth plots taken at fixed q^2. The two most frequently used form factors $G_E(q^2)$ and $G_M(q^2)$, the "Sachs" form factors (Ref. [7]), are linear combinations of the formerly used Dirac and Pauli form factors F_1, F_2

$$G_E(q^2) = F_1(q^2) + \frac{q^2}{4M_P^2} F_2(q^2),$$
$$G_M(q^2) = F_1(q^2) + F_2(q^2) \qquad (2)$$

(M_P: mass of the proton) restricted to

$$G_E(q^2 = 0) = 1, \quad G_M(q^2 = 0) = 0.$$

Using G_E and G_M is of greater algebraic convenience when extracting form factors from the Rosenbluth formula.

$$A(q^2) = \left[G_E^2(q^2) + \frac{q^2}{4M_P^2} \cdot G_M^2(q^2)\right] \Big/ \left(1 + \frac{q^2}{4M_P^2}\right),$$
$$B(q^2) = 2 \cdot \frac{q^2}{4M_P^2} G_M^2(q^2). \qquad (3)$$

2. Electron-Neutron Scattering

This has been investigated in three kinds of experiments:

a) The scattering of slow neutrons by atomic electrons. This experiment is very crucial to the slope of the electric form factor of the neutron at $q^2 = 0$

$$dG_{EN}/dq^2\big|_{q^2=0}.$$

b) Elastic electron-deuteron scattering. Because of the lack of a pure neutron target the form factors of the neutron are determined by elastic electron-deuteron scattering. The deuteron is the simplest nucleon system and well-known in the non-relativistic approach. With increasing momentum transfer the uncertainties in the calculations (theory) of the deuteron wave functions are greater than the statistical errors of the experiments. Therefore the form factor values are affected by an additional large systematic error.

c) Quasielastic electron-deuteron scattering. For higher momentum transfer the quasielastic electron-deuteron scattering is useful to avoid the model dependence of the deuteron wave functions. In this kind of experiment the ratio of electron-neutron and electron-proton scattering cross section can be determined directly.

III. The Hadronic Structure of the Nucleons

The information on the structure of the nucleon is contained in the shape of the momentum transfer dependence of the form factors. The proton form factors G_{EP}, G_{MP} as well as the magnetic neutron form factor G_{MN} decrease steadily with increasing q^2. The data at high q^2 imply that the proton has no hard core. This is prevealed by the q^{-4} dependence of the form factors.

Two empirical "laws" are often used to describe the q dependence. First the "scaling law" (μ: magnetic moment)

$$G_{EP}(q^2) = G_{MP}(q^2)/\mu_P = G_{MN}(q^2)/\mu_N,$$
$$G_{EN}(q^2) = 0 \qquad (4)$$

and second the phenomenological "dipole fit"

$$G_D(q^2) = \frac{1}{(1 + q^2/0.71)^2} = \frac{1}{(1 + q^2/18.23)^2},$$
$$q^2 \text{ in } (\text{GeV/c})^2, \quad q^2 \text{ in } \text{fm}^{-2},$$
$$1\ (\text{GeV/c})^2 = 25.68\ \text{fm}^{-2}, \qquad (5)$$

which describes the form factors in a convenient way with an accuracy of about 15%. At high q^2 the dipole fit gives the q^{-4} dependence, predicted by the quark model, but on the other hand it has no relevant physical meaning (Ref. [8, 9, 10]).

For the theoretical description one assumes that the nucleon is a composed system. The coupling of the virtual photon can be represented by the graph

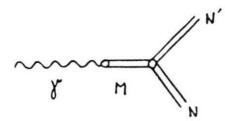

The intermediate state M indicates a meson or other hadronic particles.

In order to have well-defined quantum numbers for the t-channel exchange ($t = -q^2$, $t < 0$ in the physical, space-like region, $t > 0$ in the time-like region), one has to consider the isoscalar and

isovector combinations of proton and neutron form factors

$$G_{is}(t) = \tfrac{1}{2}(G_{iP} + G_{iN}),$$
$$G_{iv}(t) = \tfrac{1}{2}(G_{iP} - G_{iN}) \qquad (6)$$

with $i = E, M$ for the electric and magnetic part. The exchange of particles of isospin $I = 0$ (ω, Φ) belongs to G_S and those with $I = 1$ (ϱ, ϱ') to G_V.

The main approach to a physical understanding of the form factors is based on dispersion relations. In this approach the form factors are assumed to be analytic functions in the entire t-plane. The form factors at space-like momentum transfer, i.e., the region which is accessible to electron-nucleon scattering, are expressed as integrals over the imaginary part of the form factor (the spectral function) in the time-like region.

$$G(t) = \frac{1}{\pi}\int_{t_0}^{\infty} \frac{\operatorname{Im} G(t')}{t' - t}\,dt' . \qquad (7)$$

The extrapolation of the experimental form factors to the time-like region ($t > 0$) of momentum transfer can be done in a simple treatment by means of the conformal transformation technique (Reference [11]).

Physically, the spectral function is closely related to the mass spectrum of strongly interacting systems of spin and parity 1^-, baryon number and strangeness zero and of appropriate isotopic spin. The threshold t_0 is $4m_\pi^2$ for the isovector and $9m_\pi^2$ for the isoscalar intermediate states. From the vector dominance model we expect the spectral function to have peaks at the positions of the vector mesons of strangeness zero.

One tries to determine the spectral function $\operatorname{Im} G(t)$ in two ways: either by analytical continuation from the experimental data in the physical region $q^2 = -t > 0$ alone or by using in addition extended unitarity and other experimental data. In the case of the isoscalar form factors one can describe the form factors by the known meson resonances and we have found no evidence for any contribution of a non-resonant three pion state.

However, the spectral function of the isovector form factor shows a significant contribution from a non-resonant two pion state near threshold $t = (4m_\pi^2)$ in addition to the braod ϱ peak. To describe this spectral function near threshold, extracted from the experimental data, with a theoretical model, the two-pion state at threshold must be calculated with the pion nucleon scattering amplitudes in first order of perturbation theory. Because of the bigger errors in former experiments one could describe the data with simpler assumptions about the πN scattering amplitudes. In Fig. 1 we show the spectral function determined a) from the analytical extrapolation from the physical region and b) the calculated function (Ref. [11]). To obtain a consistent data set, we have reanalysed all experimental data since 1965 (Ref. [20]). The best fits via dispersion relations for the electric and magnetic proton form factors are shown in Figs. 2 and 3 (dashed lines). This dispersion relation fit describes excellently the measured form factors within the statistical errors for the whole q^2 range up to the highest q^2 values. Also the fit via dispersion relations to the electric form factor of the neutron (solid line in Fig. 4) is in very good agreement with the experimental points.

IV. Charge Density of the Nucleons

To determine the charge distribution one describes the interaction effects in terms of the matrix element of the nucleon charge and current operators.

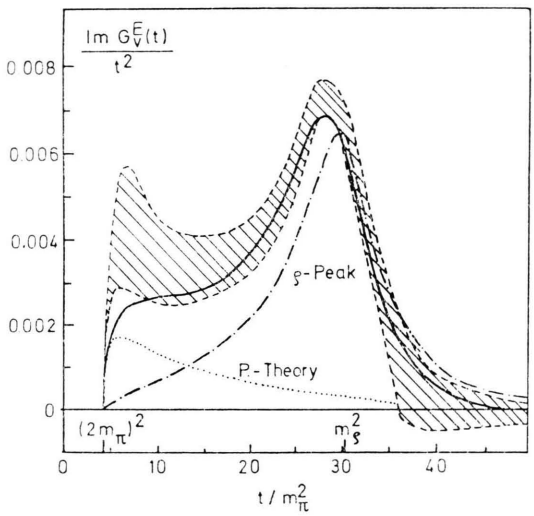

Fig. 1. The solid line shows the calculated spectral function and the hatched area denotes the uncertainty of the extrapolated spectral function. The ϱ-peak is indicated by the dashed-dotted curve and the contribution from the pion-nucleon scattering amplitudes in fiirst order perturbation theory is denoted by the dotted curve.

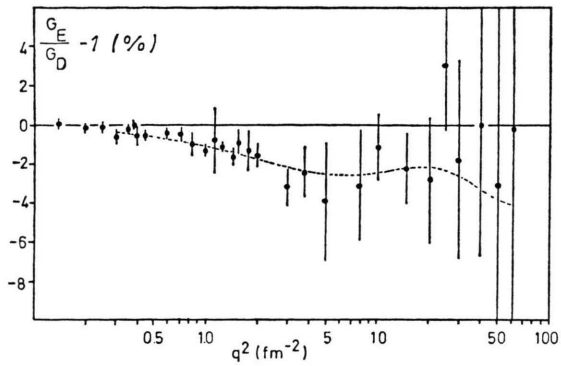

Fig. 2. The ratio of the electric form factor G_{EP} of the proton to the prediction of the dipole fit $G_D = (1 + q^2/18.23)^2$ versus q^2. The dashed line is the best fit calculated with the monopole ansatz.

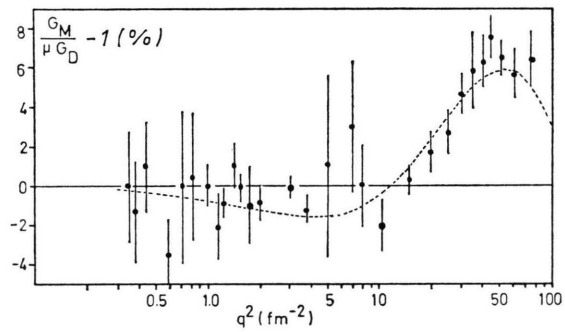

Fig. 3. The same as in Fig. 2. but for the magnetic form factor G_{MP} of the proton.

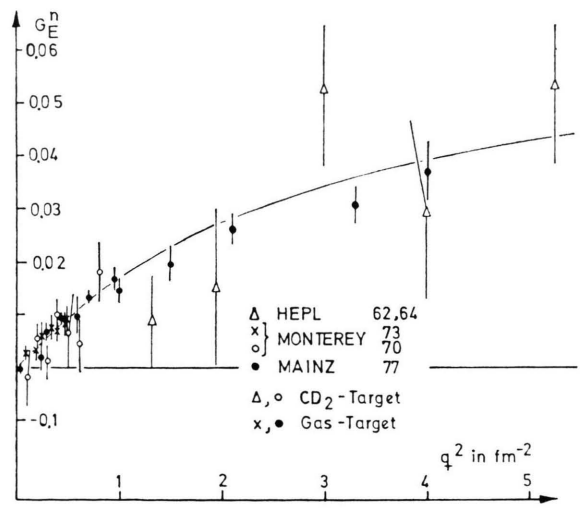

Fig. 4. The electric form factor G_{EN} of the neutron as a function of q^2. The data from different laboratories (Ref. [20]) are determined with different targets. The solid line is the calculated description with the dispersion relation.

The expansion of the space components to order $1/M$ (M is the mass of the nucleon) leads to the usual non-relativistic current operator. The zeroth component expanded to order of $1/M^2$ is given by

$$\langle \boldsymbol{p}'\,\lambda' | \hat{\varrho}(0) | \boldsymbol{p}\,\lambda \rangle = \chi^+_{\lambda'}\, \varrho(\boldsymbol{p}, \boldsymbol{q})\, \chi_\lambda ,$$
$$\varrho(\boldsymbol{p}, \boldsymbol{q}) = (1 - \boldsymbol{q}^2/8M^2)\, G_E(\boldsymbol{q}) . \tag{8}$$

$\boldsymbol{p}$ and $\boldsymbol{p}'$ are the initial and final three momenta of the nucleon, λ and λ' are the initial and final helicities of the nucleon, χ_λ is the usual two-component spin wave function, $\hat{\varrho}(0)$ is the zeroth component of the four-vector current operator at the point $\boldsymbol{x} = 0$, $t = 0$. In this approach the form factor G_E corresponds directly to the charge density. Thus we can calculate the charge density as a function of the distance from the center of the nucleon by the Fourier transform of $G_E(q^2)$. Assuming a radial distribution the transformation is given for a general form factor $F(q)$ by

$$|\boldsymbol{q}| \cdot F(|\boldsymbol{q}|) = 4\pi \int_0^\infty \varrho(r) \cdot \sin(|\boldsymbol{q}| \cdot |\boldsymbol{r}|) \cdot |\boldsymbol{r}| \cdot \mathrm{d}|\boldsymbol{r}| ,$$
$$|\boldsymbol{r}| \cdot \varrho(|\boldsymbol{r}|) = \frac{1}{2\pi^2} \int_0^\infty F(|\boldsymbol{q}|) \cdot \sin(|\boldsymbol{q}| \cdot |\boldsymbol{r}|) \cdot |\boldsymbol{q}| \cdot \mathrm{d}|\boldsymbol{q}| , \tag{9}$$

where the normalization condition is

$$4\pi \int_0^\infty \varrho(r)\, r^2\, \mathrm{d}r = 1 . \tag{10}$$

To calculate this integral one needs data points in the whole momentum region. Because of the experimental limitation of the measured q-region, we can determine the charge distribution with a spatial resolution only of the order $1.5/q = 0.15$ fm for $q^2 = 100$ fm^{-2}. In the case of electron-nucleon scattering there exists an additional stronger limitation arising from the recoil of the nucleon during the scattering process.

1. The Fourier transformation (Eq. (9)) exists only for the three momentum transfer. In order to take into account the recoil of the nucleons, we use the Breit system in which the fourth component $q_0 = i\Delta E$ of the four momentum transfer vanishes. Then the Fourier transformation should be evaluated at different effective momentum transfers q. These changes can be taken into account by a kinematical transformation.

2. The relation between the charge distribution and the form factor (Eq. (9)) can only be calculated in the non-relativistic limit. For high momentum transfer $q^2 = 8M^2 = 180\ \mathrm{fm}^{-2}$ this approach is not valid and therefore the Fourier transform can not be discussed in terms of charge distribution.

3. In the case of electron nucleon scattering we have not a pure Coulomb scattering (see Equation (1)). The subtraction of the magnetic part can be done by the method of Rosenbluth plots in principle. For large momentum transfer the contribution of the magnetic scattering to the cross section increases rapidly with increasing q^2. If we assume an uncertainty of 5% typical for a large q^2 experiment, we cannot separate reliably the form factors by Rosenbluth plots for q^2 values higher than $100\ \mathrm{fm}^{-2}$.

Because of these limitations, the spatial resolution of the charge distribution is strongly restricted. To get an illustration of the charge distribution in the coordinate space of the nucleon, we have made the attempt to calculate the Fourier transform while respecting the limitation discussed above.

In the case of the nucleus the determination of the density should lead to definite statements about the change density in coordinate space. This procedure has the disadvantage that $\varrho(r)$ can only be determined with some assumptions. This is obvious from the Born approximation, where lack of data beyond the maximum momentum transfer of the experiment $q(\max)$ immediately implies total ignorance of all Fourier components above $q(\max)$.

In principle the Fourier transform can be calculated for each value of r (method 1). In this procedure the q-dependence of the form factors has to decrease more rapidly than q^{-2} to produce convergence of the integral (Eq. (9)). In addition for $r \to 0$ it is necessary to demand a q-dependence of the order q^{-4}. Furthermore it is necessary to interpolate between measured form factor values.

Ansatzes for the form factors can be taken from the dispersion relation analysis, discussed above (method 2). The q-dependence of the form factor is mainly given by the position and the coupling constant of the poles (ϱ, ω, Φ etc.) in the time-like region. For large momentum transfer, the poles corresponding to large masses dominate the q dependence whereas in the low q region the data are sensitive to the pole-position corresponding to small masses. Therefore the high q data can be described by a dipole fit because the corresponding mass values of the poles in this region show only a relative small mass difference and furthermore the assumption of the q^{-4} dependence of the form factor can be taken into account by such an ansatz. The Fourier transform gives an exponential fit.

For the intermediate momentum region the relative mass distance of the poles in the corresponding time-like region increases with increasing mass values. Therefore we assume a monopole ansatz which corresponds to a Yukawa fit. These relations are shown in Table 1. The two ansatzes are useful for a rough interpolation and they provide a simple treatment of the Fourier transform. The high-accuracy experimental data at low q^2 and the theoretical calculation of the spectral function have shown that these ansatzes are too rough for a good description of the data. The deviation of the exact calculation with the lowest pole, the ϱ pole near threshold, is shown in Figure 1. Because of this result, the Fourier transform calculated by Yukawa- or exponential or Gauss fits cannot describe the form factor data in the whole measured q region very well. In our analysis, we have used the dispersion fit including the strong enhancement of the spectral function near threshold.

A useful parametrization of the charge density of the nucleus is given by the Fourier Bessel analysis (Ref. [19]) (method 3). In this case $\varrho(r)$ is approximated by the series

$$r \cdot \varrho(r) = \sum_{\nu=1}^{\infty} a_\nu \cdot \sin\left(\frac{\pi}{R}\,\nu\, r\right), \quad r \leqq R,$$
$$r \cdot \varrho(r) = 0, \qquad r > R, \qquad (11)$$

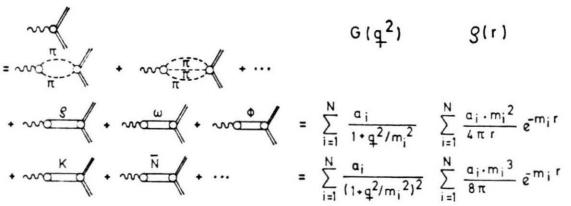

Table 1. The coupling mechanism of the electromagnetic field to the strong interacting hadron. The development of the one photon exchange graph in a series of non-resonant π-N graphs, resonant vector meson graphs and other hadronic graphs and the corresponding form factor ansatzes as well as their Fourier transforms $\varrho(r)$ are shown.

where

$$4\pi \int_0^\infty \varrho(r)\, r^2\, \mathrm{d}r = 1\,.$$

The form factor can be described by

$$q \cdot F(q) = 4\pi \sum_{\nu=1}^{\infty} \left(\frac{\pi}{R}\nu\right) a_\nu (-1)^\nu \frac{\sin(qR)}{q^2 - \left(\frac{\pi}{R}\nu\right)^2} \quad (12)$$

where

$$F(q^2 = 0) = 1\,, \quad F\left(q \to \frac{\pi}{R}\nu\right) = \frac{2R^2}{\nu} a_\nu\,.$$

The coefficients a_ν are mainly determined by the form factor data around $q = (\pi/R)\nu$. The parameter R was chosen in such a way, that χ^2/D.F. is not changed significantly by changing R to higher values. The lowest value is $R = 4$ fm for the proton and neutron. For high q data we have used the dipole fit (Eq. (5)). An additional amplitude factor was fixed at the form factor value for the largest momentum transfer q(max) and the error bars were chosen to be of the same size as the calculated form factor values. The results of the calculated charge distributions are shown in Figs. 5—7 for the proton and the neutron respectively. The error bands include the statistical errors and the uncertainties arising from the model dependence.

V. The RMS Radii of the Nucleons

The advantage of low q^2 measurements is that the data are very crucial to the determination of the rms radii of the nucleons. The radius could be determined with a small systematic error. This was possible mainly by reducing the normalization error arising from the target thickness. The nucleon radii are calculated from the slope of the q dependence of the form factor at the photon point $q^2 = 0$

$$\langle r^2 \rangle = -\frac{6}{G(q^2=0)} \frac{\mathrm{d}G(q^2)}{\mathrm{d}q^2}\bigg|_{q^2=0}\,. \quad (13)$$

Usually one determines the slope by some analytical description of the form factors up to $q^2 = 0$. Therefore one has to assume, that the selected representation is valid also outside the region of measurements near the point $q^2 = 0$. In particle physics, one ussually uses for this purpose phenomenological parametrizations. In nuclear physics, more complicated forms of charge distribution and of corresponding form factors are used. This procedure is sensitive to the analytical ansatz and, therefore, model dependent. To reduce the model dependence, we use the Taylor expansion of the form factors which leads to a specific form of them. This procedure assumes certain analytic properties of the form factor in the t-plane. Thus this model indepent method is restricted in the q^2-region, while the region of convergence of the Taylor expansion in the t-plane is limited by location of the nearest singularity $|t| \leqq t_0 = 4m_\pi^2 \approx 2\,\mathrm{fm}^{-2}$. Because of the large number of high accuracy data measured at Mainz, Orsay and Saskatoon (Ref. [20]), we could determine the rms charge radius of the proton to: $\langle r_{\mathrm{EP}}^2 \rangle^{1/2} = 0.862(12)$ fm. The magnetic proton radius has a greater uncertainty, because of the lack of measurements at backward angles: $\langle r_{\mathrm{MP}}^2 \rangle^{1/2} = 0.858(56)$ fm. The slope of the neutron charge form factor was measured by scattering of slow neutrons by atomic electrons with very high accuracy (Ref. [17, 18]):

$$\mathrm{d}G_{\mathrm{EN}}/\mathrm{d}q^2\big|_{p^2=0} = 1.95(3) \cdot 10^{-2}\,\mathrm{fm}^2.$$

In the case of the magnetic neutron radius we have not found a significant difference from the magnetic proton radius: $\langle r_{\mathrm{MN}}^2 \rangle^{1/2} = 0.876(70)$ fm.

The value of the rms radius is very important in the calculation of the Lamb shift. The main theoretical contribution to the Lamb shift

$$S = \Delta E(2S_{1/2}) - \Delta E(2P_{1/2})$$

in a hydrogen-like system arises in the lowest order from self energy and vacuum polarization corrections. In Ref. [12] the calculations of the lower order terms are summarized. An additional well-known correction to the Lamb shift arises from fourth order radiative corrections, reduced mass effects, relativistic recoil corrections, and the effect of nuclear size. The non-relativistic size correction is proportional to $R^2 = \langle r^2 \rangle$, which can be determined by experiments on muonic atoms and by electron scattering experiments. In the case of hydrogen, only the latter information is presently available. The recent analysis of the electron-proton elastic scattering data yields 0.862(12) fm. This value is larger than the dipole fit value, 0.811 fm, which has been generally used in evaluating the Lamb shift in hydrogen (Ref. [12, 13, 14, 15]).

The difference $\Delta R = 0.051$ fm produces a change in the theoretical value for the Lamb shift of 0.02 MHz, which is at the level of precision of the

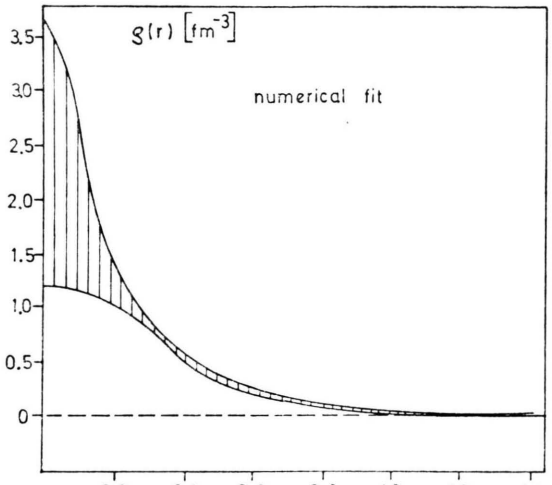

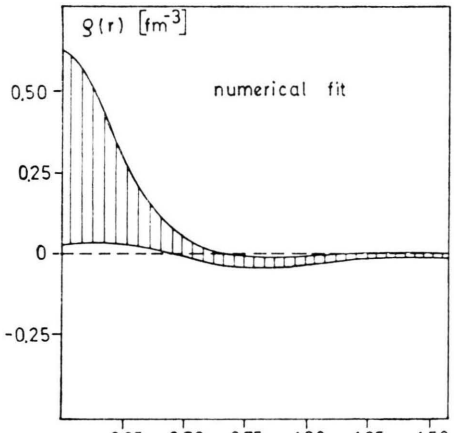

Fig. 5

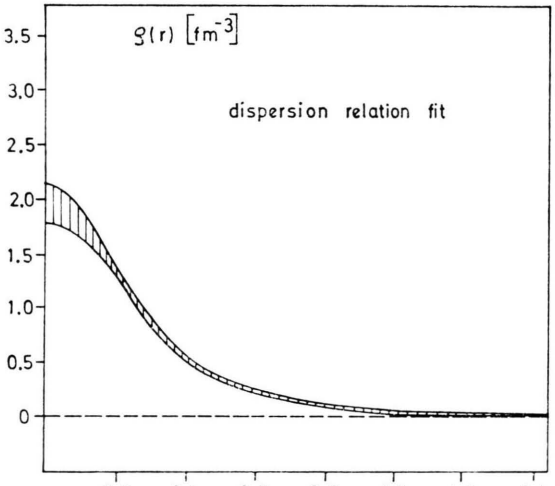

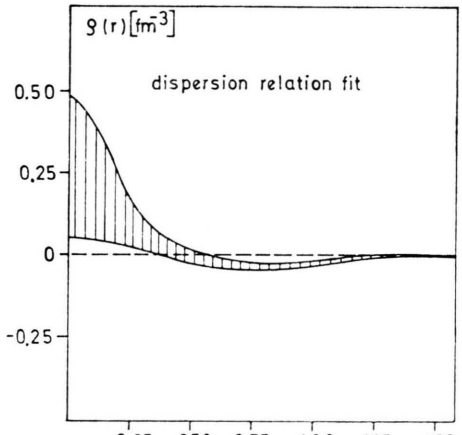

Fig. 6

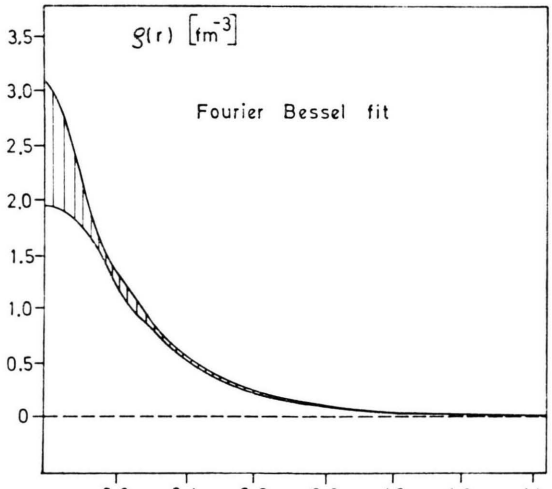

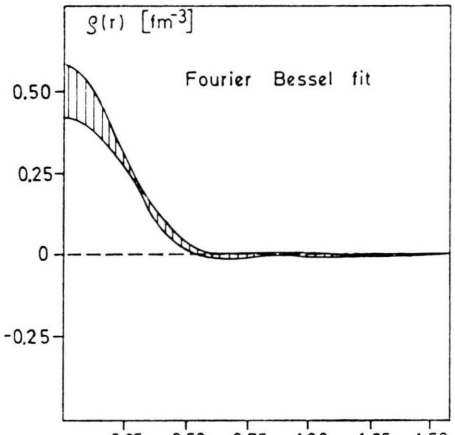

Fig. 7

Figs. 5—7. The charge densities of proton (left hand side) and neutron (right hand side) calculated with a numerical fit (Fig. 5), dispersion relation fit (Fig. 6), Fourier Bessel fit (Fig. 7). The hatched area denotes the uncertainty of the experimental data as well as the model dependence.

recent experiment (Ref. [16]). Assuming $R = 0.862$ fm, the theoretical value with an estimated uncertainty for uncalculated terms, is (Ref. [12, 13])

$$S(\text{theor}) = 1057.885(10)\ \text{MHz} \quad \text{with}$$
$$R = 0.862\ \text{fm},$$

$$S(\text{theor}) = 1057.865\ \text{MHz} \quad \text{with}$$
$$R = R(\text{dipole}).$$

Lundeen and Pipkin (Ref. [16]) using the separate oscillator field method to produce a resonance narrower than the line width, have obtained

$$S(\text{exp}) = 1057.893(20)\ \text{MHz}$$

which agrees very well with the theoretical value, if we assume the revised rms radius of the proton.

We would like to thank the entire laboratory staff of the Institut für Kernphysik, Universität Mainz, for the excellent overall support. We are indebted to Prof. P. Brix, Max-Planck-Institut für Kernphysik Heidelberg, for stimulating us to make an analysis of the e-p and e-d data in terms of charge densities.

[1] F. Gutbrod and G. Hartmann, Z. Phys. C **2**, 153 (1979).
[2] G. Höhler and E. Pietarinen, Nucl. Phys. B **95**, 210 (1975).
[3] M. Gourdin, Phys. Reports **11**, 29 (1974).
[4] V. B. Berestetskii and M. V. Tetent'ev, Sov. J. Nucl. Phys. **25** (No. 3), 347 (1977).
[5] G. G. Simon, Ch. Schmitt, F. Borkowski, C. Ottermann, V. H. Walther, D. Bender, and A. von Gunten, Nucl. Instrum. Meth. **158**, 185 (1979).
[6] G. G. Simon, Ch. Schmitt, F. Borkowski, and V. H. Walther, Internal Report KPH 12/79 and Nucl. Phys. A 333,381 (1980).
[7] R. G. Sachs, Phys. Rev. **126**, 2256 (1962). — M. N. Rosenbluth, Phys. Rev. **79**, 615 (1950).
[8] F. Borkowski, G. G. Simon, V. H. Walther, and R.D. Wendling, Z. Phys. A **275**, 29 (1975).
[9] F. Borkowski, G. G. Simon, V. H. Walther, and R. D. Wendling, Nucl. Phys. B **93**, 461 (1975).
[10] F. Borkowski, P. Peuser, G. G. Simon, V. H. Walther, and R. D. Wendling, Nucl. Phys. A **222**, 269 (1974).
[11] G. Höhler, E. Pietarinen, I. Sabba-Stefanescu, F. Borkowski, G. G. Simon, V. H. Walther, and R. D. Wendling, Nucl. Phys. B **114**, 505 (1976).
[12] B. E. Lautrup, A. Peterman, and E. de Rafael, Phys. Reports **3**, 193 (1972).
[13] G. W. Erikson and D. R. Yennie, Ann. Phys. New York **35**, 271, 447 (1965).
[14] G. W. Erikson, Phys. Rev. Lett. **27**, 780 (1971).
[15] P. J. Mohr, Phys. Rev. Lett. **34**, 1050 (1975).
[16] S. R. Lundeen and F. M. Pipkim, Phys. Rev. Lett. **34**, 1368 (1975).
[17] V. E. Krohn et al., Phys. Rev. D 8, 1305 (1973).
[18] L. Koester et al., Phys. Rev. Lett. **36**, 1021 (1976).
[19] B. Dreher, J. Friedrich, K. Merle, H. Rothhaas, and G. Luehrs, Nucl. Phys. A **235**, 219 (1974).
[20] G. Höhler, I. Sabba-Stefanescu, F. Borkowski, G. G. Simon, V. H. Walther, and R. D. Wendling, Compilation of Electron-nucleon Scattering Data and Nucleon Form Factors, Karlsruhe-Mainz Report 1976.